

STATE MEASUREMENT BY PHOTON FILTERING IN A RING CAVITY

G. M. D'ARIANO, L. MACCONE, M. G. A. PARIS and M. F. SACCHI

*Theoretical Quantum Optics Group, INFN and Dipartimento di Fisica “Alessandro Volta”
Università di Pavia, via A. Bassi 6, I-27100 Pavia, Italy*

Received 8 December 1999

We suggest a method for measuring the photon number distribution and the density matrix of a single-mode radiation field. The setup consists of a chain of active ring cavities, each fed by a strong coherent probe and coupled to the signal through cross-Kerr phase modulation. Each cavity is set at resonance by a different Fock component of the signal, so that the detection probability at the cavities output is proportional to the signal photon statistics. The off-diagonal elements of the density matrix can be evaluated by measuring the photon statistics of a set of displaced signal states. The suggested setup allows a reliable state measurement even with low quantum efficiency at detectors.

1. Introduction

The detailed photon number distribution of the radiation state $\hat{\rho}$ cannot be easily measured by direct photodetection, since the current technology provides detectors with mutually exclusive limitations: a linear detector with high quantum efficiency works only with large photon fluxes, whereas high sensitive avalanche photodetectors are nonlinear and have limited quantum efficiency. In any case, there is no available high-efficiency photodetector which can discriminate a single photon in a range of, say, ten photons.

For the above reasons, the homodyne tomography technique^{1,2} has become a popular method for reconstructing the photon number distribution,^{3,4} because the amplification from the local oscillator in the homodyne detector allows one to use high-efficiency linear photodiodes. Other methods have also been suggested² to overcome the inherent inadequacy of photodetectors, either by photon “chopping”⁵ or by mixing the signal mode with a strong local oscillator, such as in unbalanced^{6,7} and multiphot⁸ homodyne detection schemes. Further proposals⁹ involve indirect measurements that exploit the interactions of the field with atomic degrees of freedom. All these methods have some limitations which, so far, prevented their full implementation for the reconstruction of the radiation state. In particular, they suffer from the detrimental effects of non-unit quantum efficiency. Indeed, quantum homodyne tomography plays a privileged role, since it is the best method for

arbitrary state reconstruction which has been implemented so far.^{4,10} On the other hand, homodyne tomography itself suffers from statistical errors which rapidly increase, versus the index n of the photon number distribution $P(n) = \langle n | \hat{\rho} | n \rangle$, even for high values of quantum efficiency, thus needing large samples of experimental data. In the above scenario, it becomes very interesting to devise a detection method where the quantum efficiency is not a critical parameter. This is the case of the setup that we present in this paper, which, in principle, can measure the photon distribution of a given signal with a relatively small number of data, and with little dependence on quantum efficiency at photodetectors. As we will show, by enlarging the data sample, the setup also allows us to reconstruct the off-diagonal density-matrix elements through the least-squares method of Ref. 7, by measuring the photon distribution of a set of displaced signal states. Remarkably, the resulting state-reconstruction method also works at low quantum efficiency.

2. Dynamics of the Kerr Cavity

The device is schematically depicted in Fig. 1. It consists of a certain number of active ring cavities, each fed by a strong coherent probe and coupled to the signal density operator $\hat{\nu}$ by a nonlinear medium that imposes cross-Kerr interaction. Notice that the signal mode does not interact with the cavity mirrors, but simply imposes a phase-shift due to the Kerr medium, thus, it is not affected by the losses caused by the mirrors. The effect of losses in high-Q cavities is scarcely relevant for the excited coherent states therein. On the other hand, the signal decoherence that is induced only by the Kerr medium imposes limits to the number of concatenated cavities.

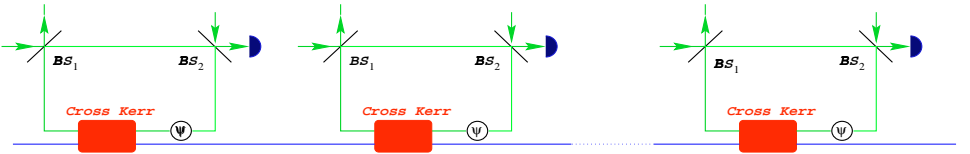


Fig. 1. Schematic diagram of the setup to measure the photon number distribution of a generic input signal $\hat{\nu}$. Each cavity is fed by a strong coherent probe and coupled to the signal by a nonlinear medium that imposes cross-Kerr phase modulation. The cavities can be separately tuned by adjusting the phase shift ψ_k . In this way, each cavity is set at resonance by a different Fock component N_k in the signal state, and the detection probability $P_1^{(k)}$ at the output of the k th cavity is proportional to the diagonal matrix element $\nu_{N_k N_k}$ of the signal.

Each cavity can be separately tuned by adjusting the phase shift ψ_k . In this way, each cavity is set at resonance by a different Fock component $|N_k\rangle$ in the signal state, and, as shown in the following, the detection probability $P_1^{(k)}$ at the output of the k th cavity is proportional to the diagonal matrix element $\nu_{N_k N_k}$ of the signal state.

Let us first consider the dynamics of a single cavity. The input and output modes of the cavity (a_j and b_j , respectively, $j = 1, 2$) are connected through the linear transformation

$$\begin{cases} b_1 = \kappa(\varphi)a_1 + e^{i\varphi}\sigma(\varphi)a_2 \\ b_2 = \sigma(\varphi)a_1 + \kappa(\varphi)a_2 \end{cases}, \quad (1)$$

where φ is the total phase shift suffered by the cavity mode. In Eq. (1), the amplitude of the phase-dependent transmissivity σ and reflectivity κ are given by

$$\kappa(\varphi) \doteq \frac{\sqrt{1-\tau}(e^{i\varphi}-1)}{1-[1-\tau]e^{i\varphi}}, \quad \sigma(\varphi) \doteq \frac{\tau}{1-[1-\tau]e^{i\varphi}}, \quad (2)$$

with $|\kappa(\varphi)|^2 + |\sigma(\varphi)|^2 = 1$, τ being the transmissivity of the cavity beam splitters. In our case, the phase φ is the sum of the shift due to the Kerr modulation and the tunable phase ψ . The Kerr interaction is governed by the evolution operator $U_K = \exp\{i\chi t a^\dagger a b^\dagger b\}$, a and b being the signal and the cavity modes, respectively, and χt the overall Kerr coupling. Each Fock component $|n\rangle$ of the signal imposes to the cavity mode a total phase shift $\varphi \equiv \varphi_n = \psi - \chi n t$. It is clear that by adjusting the value of ψ to $\psi = \chi t n^*$, we can select which Fock component $|n^*\rangle$ sets the cavity at resonance. To simplify the notation, we write $\sigma_n \doteq e^{i\varphi_n}\sigma(\varphi_n)$ and $\kappa_n = \kappa(\varphi_n)$. We also assume that the coherence time of the input signal is of the order of the photon flight time in the cavity, thus assuring that the cavity mode effectively couples with the signal through the cross-Kerr medium.

The device is composed of a chain of cavities, as shown in Fig. 1. The input state before each of the cavities is given by

$$\hat{\rho}_{\text{in}} = |\alpha\rangle\langle\alpha| \otimes |0\rangle\langle 0| \otimes \hat{\nu}, \quad (3)$$

namely, a generic state $\hat{\nu}$ for the signal mode and a strong coherent state $|\alpha\rangle$ for the cavity probe mode, the second input port of the cavity being unexcited. The output state after each cavity can be easily written in the Schrödinger picture as

$$\hat{\rho}_{\text{out}} = \sum_{n,m=0}^{\infty} \nu_{nm} |\kappa_n\alpha\rangle\langle\kappa_m\alpha| \otimes |\sigma_n\alpha\rangle\langle\sigma_m\alpha| \otimes |n\rangle\langle m|. \quad (4)$$

The state in Eq. (4) is an entangled superposition, in which each Fock component of the signal corresponds to a different cavity response.

The measurement scheme consists in detecting whether (detector D on) or not (detector D off) any photon is present at one output port of the cavity. This ON/OFF detection strategy is described by a two-value probability operator measure

$$\hat{\Pi}_{\text{OFF}} \doteq \sum_{k=0}^{\infty} (1-\eta)^k |k\rangle\langle k|, \quad \hat{\Pi}_{\text{ON}} \doteq \hat{\mathbb{I}} - \hat{\Pi}_{\text{OFF}}, \quad (5)$$

where η denotes the quantum efficiency of the photodetector. The case of perfect photodetection (i.e. $\eta = 1$) leads to the projection operator on the vacuum

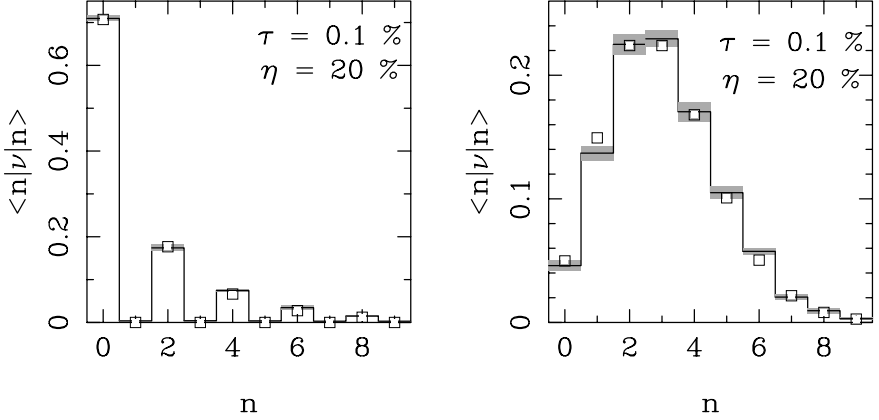


Fig. 2. Monte Carlo simulations of the whole procedure for measuring the photon number distribution. We report the distribution obtained for the input signal excited in a squeezed vacuum with $\langle a^\dagger a \rangle = 1$ average photons and a coherent state with $\langle a^\dagger a \rangle = 3$, respectively. The simulated sample consists of ten blocks of 200 data each, for a total number of $N = 2000$ repeated preparations of the signal. The quantum efficiency and the beam-splitter transmissivity are $\eta = 20\%$ and $\tau = 0.1\%$, respectively. The Kerr coupling is $\chi t = 0.1$, and the probe amplitude is $|\alpha| = 10$. Gray-shaded areas denote statistical errors, and the empty squares represent theoretical values.

$\hat{\Pi}_{\text{OFF}} = |0\rangle\langle 0|$. The probabilities corresponding to the “click” (detector D on) and to the “no-click” (detector D off) events are given by

$$P_{\text{ON}} = \text{Tr}[\hat{\Pi}_{\text{ON}}\hat{\rho}_{\text{out}}] = \sum_{n=0}^{\infty} \nu_{nn} \left(1 - e^{-\eta|\alpha|^2 |\sigma_n|^2}\right) \quad (6)$$

$$P_{\text{OFF}} = \text{Tr}[\hat{\Pi}_{\text{OFF}}\hat{\rho}_{\text{out}}] = \sum_{n=0}^{\infty} \nu_{nn} e^{-\eta|\alpha|^2 |\sigma_n|^2}, \quad (7)$$

whereas the conditional output states are given by

$$\hat{\nu}_{\text{ON}} = \frac{e^{-|\alpha|^2}}{P_{\text{ON}}} \sum_{n,m=0}^{\infty} \nu_{nm} e^{|\alpha|^2 [\kappa_n \kappa_m^* + \sigma_n \sigma_m^*]} (1 - e^{-\eta|\alpha|^2 \sigma_n \sigma_m^*}) |n\rangle\langle m| \quad (8)$$

$$\hat{\nu}_{\text{OFF}} = \frac{e^{-|\alpha|^2}}{P_{\text{OFF}}} \sum_{n,m=0}^{\infty} \nu_{nm} e^{|\alpha|^2 [\kappa_n \kappa_m^* + (1-\eta)\sigma_n \sigma_m^*]} |n\rangle\langle m|. \quad (9)$$

The explicit form of the cavity transmissivity function is given by

$$|\sigma_n|^2 = \left[1 + 4 \frac{1-\tau}{\tau^2} \sin^2 \frac{\psi - \chi n t}{2} \right]^{-1}, \quad (10)$$

which exhibits a periodic structure sharply peaked at

$$n = \frac{\psi + 2\pi j}{\chi t} \doteq n^* + \frac{2\pi}{\chi t} j, \quad j \in \mathbb{N}, \quad (11)$$

with unit maximum height and width of the same order of the beam splitter transmissivity τ (typically $\tau \sim 0.1\% \div 0.01\%$). The value n^* can be adjusted to an arbitrary integer by tuning the phase shift ψ as a multiple of χt . On the other hand, subsequent integers that satisfy Eq. (11) for $j \neq 0$ play no role when they correspond to Fock components that are not excited in the input signal [for nonlinearity shift $\chi t \ll 1$, this is true for not too excited input states with $\langle \widehat{\Delta n^2} \rangle \ll 2\pi/(\chi t)$]. In this case, the detection probability rewrites as

$$P_{\text{ON}} \simeq \nu_{n^*n^*} \left[1 - e^{-\eta|\alpha|^2} \right] + \frac{\eta|\alpha|^2\tau^2}{(\chi t)^2} \sum_{k \neq n^*} \frac{\nu_{kk}}{(n^* - k)^2}. \quad (12)$$

Equation (12) indicates that for a cavity with high quality factor (i.e. $\tau \ll \chi t$), the detection probability is proportional to the selected diagonal matrix element $P_{\text{ON}} \simeq \nu_{n^*n^*} [1 - \exp(-\eta|\alpha|^2)]$. Correspondingly, for low values of the nonlinearity, the conditional output states are

$$\hat{\nu}_{\text{OFF}} \simeq \sum_{n \neq n^*} \frac{\nu_{nn}}{P_{\text{OFF}}} |n\rangle\langle n| \quad \hat{\nu}_{\text{ON}} \simeq |n^*\rangle\langle n^*|. \quad (13)$$

In summary, the detection probability is proportional to the selected diagonal matrix element, and a successful photodetection reduces the signal to the corresponding Fock number state.

3. The Measurement Scheme

Here, we are interested in measuring the whole photon number distribution of a given signal. Therefore, we use a chain of cavities, each tuned at a different integer N_k . The measurement scheme consists of repeatedly preparing the signal and then detecting which cavity is switched on. The relative frequency of “clicks” for the k th cavity is proportional to the diagonal matrix element $\nu_{N_k N_k}$ of the signal. In doing this, it should be taken into account that the input signal $\hat{\nu}^{(k)}$ of the k th cavity is the output signal from the $(k-1)$ th one, namely, the state that has been reduced according to the outcome of the $(k-1)$ th photodetector. Hence, for the detection probability $P_{\text{ON}}^{(k)}$ at the output of the k th cavity we have

$$P_{\text{ON}}^{(k)} \simeq \nu_{N_k N_k}^{(k)} \left[1 - \exp(-\eta|\alpha|^2) \right], \quad (14)$$

where the matrix elements, after the reduction, due to the $(k-1)$ th detection are given by the recursion formula

$$\nu_{pp}^{(k)} = \begin{cases} \delta_{pN_{k-1}} & \text{if } D^{(k-1)} \text{ is ON} \\ \nu_{pp}^{(k-1)} \frac{1 - \delta_{pN_{k-1}}}{P_{\text{OFF}}^{(k-1)}} & \text{if } D^{(k-1)} \text{ is OFF} \end{cases}. \quad (15)$$

In order to check the reliability of the present measurement scheme, we have performed several Monte Carlo simulations of the whole detection strategy. In Fig. 2, we report the photon distribution obtained for the input signal excited in a squeezed vacuum and a coherent state, respectively. Remarkably, the photon distribution has been reconstructed with a simulated sample of only $N = 2000$ repeated preparations of the signal, and with low quantum efficiency of the probe photodetectors ($\eta = 20\%$). Indeed, the most relevant feature of the present scheme is that the quantum efficiency of the probe photodetectors at the output of the cavities is not a critical parameter. Low quantum efficiency does not affect the quality of the reconstruction, but only decreases the overall detection rate, namely, the number of samples that activate at least one of the cavities. Notice that the detection rate could, in principle, be restored by increasing the probe amplitude α , however with the restriction that the quantity $(\eta|\alpha|^2\tau^2)/(\chi t)^2 \ll 1$ in Eq. (12).

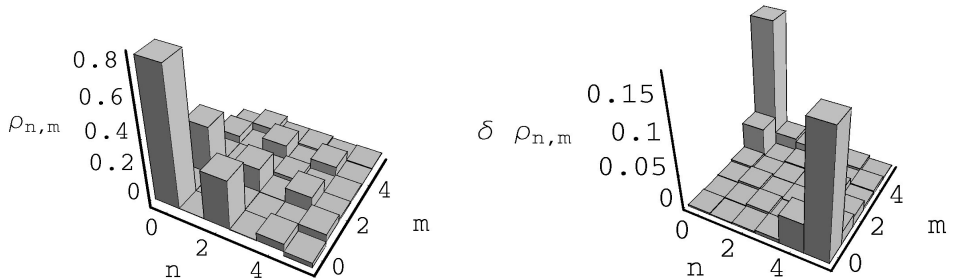


Fig. 3. Monte Carlo simulation of the reconstruction of a squeezed vacuum state with $\langle a^\dagger a \rangle = 0.5$ average photons: real part of the matrix elements (on the left), and corresponding statistical errors (on the right). The ring-cavity method has been used to measure the displaced photon number distributions $p_n(z)$, with $|z| = 1.4$ and 25 equally spaced phases $\phi = \arg z \in [0, 2\pi)$ with 4000 data each. Ten blocks have been used to evaluate statistical errors. The parameters of the setup are the following: quantum efficiency $\eta = 20\%$, beam-splitter transmissivity $\tau = 0.01\%$, Kerr coupling $\chi t = 0.1$, probe amplitude $|\alpha| = 10$.

One can also imagine the chain of cavities designed as a loop with only one cavity, with the signal from the output fed into the output many times, each time varying the tunable phase shift ψ , and continuing this process until the photodetector clicks. Such a loop needs, of course, a fast and well-synchronized tuning of the phase ψ .

The proposed setup also allows the evaluation of the off-diagonal elements of the density matrix. As shown in Ref. 7, the displaced Fock-state probability distribution $p_n(z) = \langle n, z | \hat{\rho} | n, z \rangle$, with $|n, z\rangle = e^{za^\dagger - \bar{z}a} |n\rangle$, can be used to reconstruct the density matrix $\hat{\rho}$ by means of a least-squares inversion method. The displacement parameter z can be kept constant in modulus, varying only the phase of the local oscillator that realizes the displacement on the signal $\hat{\rho}$ through a high-transmissivity beam splitter. The distributions $p_n(|z|e^{i\varphi})$ at different phases φ can then be measured by the ring-cavity method described above. In Fig. 3, we report the result for the reconstruction of a squeezed vacuum state with average photon number $\langle a^\dagger a \rangle = 0.5$,

together with the corresponding statistical errors. We stress that the reconstruction of the whole density matrix has been carried out using quantum efficiency as low as $\eta = 20\%$. We remember that the good cavity condition $\sqrt{\eta}|\alpha|\tau \ll \chi t$ poses severe limitations on the size of the nonlinear phase-shift χt . However, values as large as $\chi t = 0.1$, as in our computer simulations, have been predicted theoretically,¹¹ and are now entering into the realm of experiments.¹²

4. Conclusion

We have suggested a scheme that, in principle, allows us to measure the photon number distribution of the radiation field. The scheme is composed of a chain of ring cavities pumped with strong coherent states and coupled to the signal mode through a Kerr medium. Conventional ON/OFF photodetectors measure the probe field exiting each cavity. Through Monte Carlo simulations, we have shown that the method allows us to measure the photon distribution with high reliability, even with a limited number of input data samples and low quantum efficiency. The same setup, with the help of the least-squares inversion method of Ref. 7 applied to a set of displaced copies of the input state, can be used to measure the density matrix of a generic input signal with essentially no detrimental effect from non-unit quantum efficiency.

Acknowledgments

This work is co-sponsored by MURST under the project "Amplificazione e rivelazione di radiazione quantistica". G. M. D'Ariano thanks M. Brune for the interesting discussions. M. G. A. Paris thanks *Accademia Nazionale dei Lincei* for partial support, and O. Haderka and M. Hendrych for the interesting discussions.

References

1. G. M. D'Ariano, in *Quantum Optics and the Spectroscopy of Solids*, ed. T. Hakioglu *et al.* (Kluwer, Dordrecht, 1997), pp. 175–202.
2. D.-G. Welsch, W. Vogel and T. Opatrny, *Progr. in Opt.* **39**, in press (1999).
3. M. Munroe, D. Boggavarapu, M. E. Anderson and M. G. Raymer, *Phys. Rev.* **A52**, R924 (1995).
4. J. Mlynek, G. Breitenbach and S. Schiller, *Phys. Scr.* **T76**, 98 (1998).
5. H. Paul, P. Torma, T. Kiss and I. Jex, *Phys. Rev. Lett.* **76**, 2464 (1996).
6. K. Banaszek and K. Wodkiewicz, *Phys. Rev. Lett.* **76**, 4344 (1996).
7. T. Opatrny and D.-G. Welsch, *Phys. Rev.* **A55**, 1462 (1997).
8. A. Zucchetti, W. Vogel and D.-G. Welsch, *Phys. Rev.* **A54**, 856 (1996); M. G. A. Paris, A. Chizhov and O. Steuernagel, *Opt. Commun.* **134**, 117 (1997); M. Brune, S. Haroche, V. Lefevre, J. M. Raimond and N. Zagury, *Phys. Rev. Lett.* **65**, 976 (1990).
9. K. Jacobs, P. L. Knight and V. Vedral, *J. Mod. Opt.* **44**, 2427 (1997); S. Schneider, A. M. Herkommer, U. Leonhardt and W. P. Schleich, *J. Mod. Opt.* **44**, 2333 (1997); C. T. Bodendorf, G. Antesberger, M. S. Kim and H. Walther, *Phys. Rev.* **A57**, 1371 (1998).

10. D. T. Smithey, M. Beck, M. G. Raymer and A. Faridani, *Phys. Rev. Lett.* **70**, 1244 (1993).
11. H. Schmidt and A. Imamoglu, *Opt. Lett.* **21**, 1936 (1996); *ibid.* **23**, 1007 (1998).
12. Q. A. Turchette, C. J. Hood, W. Lange, H. Mabuchi and H. J. Kimble, *Phys. Rev. Lett.* **75**, 4710 (1995); L. V. Hau, S. E. Harris, Z. Dutton and C. H. Behroozi, *Nature* **397**, 594 (1999).